Articles   Antenna & High Frequency Research Centre

2013-10-04

Leveraging Depolarization to Increase the Link Reliability for Wireless Sensors Operating in Hyper-Rayleigh Environments

Jeff Frolik
University of Vermont, jfrolik@uvm.edu

Vit Sipal
Technological University Dublin, vit.sipal@tudublin.ie

David J. Edwards
University of Oxford, david.edwards@eng.ox.ac.uk

Recommended Citation

Leveraging Depolarization to Increase the Link Reliability for Wireless Sensors Operating in Hyper-Rayleigh Environments

Jeff Frolik, *Senior Member, IEEE*, Vit Sipal, *Student Member, IEEE*, and David J. Edwards

Abstract— **Wireless communications within enclosed environments such as aircraft and vehicles have been shown to experience fading with statistics that are worse than Rayleigh. Motivated by low-cost, low-complexity systems (e.g., wireless sensors) that may be deployed in such environments, this work explores the benefits of polarization diversity using very large data sets collected over a small area and over the 5-6 GHz band. The results also demonstrate that antennas capable of capturing depolarized signal components can significantly mitigate the harshest of fading environments.**

Index Terms— **Multipath channels, Propagation measurements, Antenna diversity, Sensor networks**

I. INTRODUCTION

ADVANCES in low-cost and low-power embedded computing and wireless communication hardware is enabling the development of machine-to-machine (M2M) systems. One early example of such M2M systems are wireless sensor networks in which distributed sensor nodes collect and wirelessly send data about the physical environment for monitoring and/or control purposes. The envisioned ubiquity of M2M systems, like sensor networks, necessitates that they may be deployed in and about complex structures resulting in multipath channels. Narrow band communication links deployed in such environments can, as has been shown [1, 2], exhibit fading over frequency and space that is statistically worse than Rayleigh. Furthermore, UWB systems deployed in confined environments can result in non-functioning links, even over the shortest of distances [3, 4].

Multipath environments are known to have a depolarization effect on point-to-point wireless communications [5, 6]. Modern wireless systems exploit such depolarization through the use of multiple-polarization antenna arrays to increase channel capacity, but for energy-constrained wireless sensor applications, link reliability is of much greater concern than capacity. Currently, wireless sensor node hardware designs typically incorporate a single linear-polarization antenna; be it an onboard ceramic chip antenna, a PCB trace antenna, or an external monopole. However, sensors nodes do have the requisite computational capability, along with a received signal strength indication (RSSI) measure integrated in their wireless chipsets, to configure more sophisticated antenna designs. The results herein will hopefully motivate designers of low-cost, wireless devices (e.g., M2M, wireless sensors and RFID) to integrate more capable antenna systems on their hardware; in particular, those having multi-polarization capability (e.g., [7, 8]).

For wireless systems nominally experiencing Rician fading, depolarization increases the random/diffuse energy and decorrelates the fading seen on orthogonal branches (i.e., antennas). As a result, the fading statistics in these channels tend towards Rayleigh [9]. That is, for these environments, depolarization makes the channel fading statistically worse. Herein, we

show, through an empirical study, that for environments where the co-polarized link fading is statistically worse than Rayleigh (i.e., hyper-Rayleigh) the statistics also tend towards Rayleigh under cross-polarized conditions. That is, for these harsh environments, depolarization can *improve* the link conditions over space and frequencies. Furthermore, we demonstrate that the degree of depolarization is such that antenna polarization selection diversity (an approach readily implemented by wireless sensor hardware) is not only effective in improving the mean signal strength but also significantly reduces the fading severity thereby resulting in more reliable communication links.

II. DEPOLARIZATION RESULTS

A. Test Environment

Worse than Rayleigh channel conditions can occur when the environment creates two strong signal components that either add constructively or destructively over changes in frequency, space, or time [1]. These 'hyper-Rayleigh' channels have been measured in airframes [2], in vehicles, and have been noted in historical data collected in buildings [10]. Hyper-Rayleigh conditions can be modeled utilizing the two-wave, diffuse power (TWDP) formulation [11] where the received signal voltage, V_R, is given to be

$$V_R = \underbrace{V_1 e^{jf_1} + V_2 e^{jf_2}}_{specular} + \underbrace{\sum_{k=3}^{N} V_k e^{jf_k}}_{diffuse}. \qquad (1)$$

In (1), $V_{1,2}$ and $f_{1,2}$ represent the magnitude and phase, respectively, of up to two dominant, *specular* components, while V_k and f_k are values associated with many ($N-2$) *diffuse* (i.e., multipath) components. For $V_1 {}^1 0$ and $V_2 {}^1 0$, hyper-Rayleigh conditions exist with the worst-case, two-ray, scenario being found when there exists only two, equal waves (i.e., $V_k = 0," k$ and $V_1 = V_2$) resulting in the probability density function of the received envelope, r, being given by (2) [1].

$$f_r(r \mid V_1 = V_2, V_k = 0" k) = \frac{2r}{\rho \sqrt{4r^2 - r^4}} ; \ r \in [0,2] \qquad (2)$$

Note that with $V_2 = 0$, we find Rician channel conditions ranging ideal (when $V_k = 0," k$) to Rayleigh (when $V_1 = 0$). For all cases, f is assumed to be uniformly distributed from 0 to 2ρ.
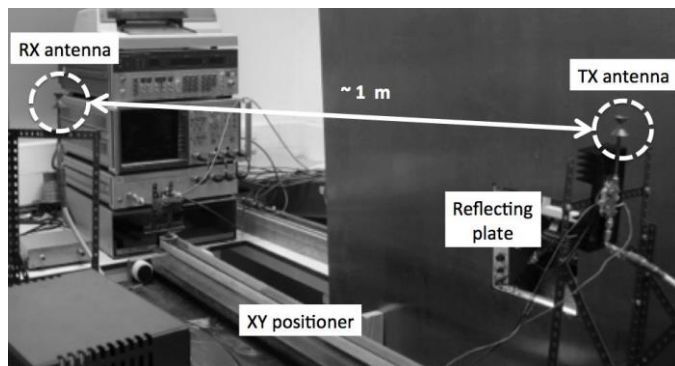

Figure 1. Short-range test setup

To emulate hyper-Rayleigh conditions in a laboratory, we created a short-range (~1 m) link having a clear line-of-sight (LOS) component and a secondary component coming off of a reflecting metal plate (Fig. 1). Bicone antennas were used and initially oriented so both the fixed-position receive antenna and the movable transmit antenna were vertically co-polarized. The transmit antenna was initially placed ~0.2 m (i.e., ~4λ) from the reflecting plate and the fixed receive antenna ~0.5 m from this surface. Across this band, the measured S_{11} performance for these antennas is less than -20 dB (Fig. 2) and the cross-polarization isolation is greater than 10 dB.

While most wireless sensor network hardware currently operates in the 2.4 GHz band, this empirical study considers the band of frequencies from 5.0 to 6.0 GHz that captures the 5.2/5.3 GHz U-NII and 5.7 GHz ISM bands. In comparison to operating in the 2.4 GHz band, operating at these higher frequencies has benefits beyond simply additional available bandwidth. Specifically, the shorter transmission range at these higher frequencies is suited to the envisioned spatially dense M2M networks and allows for greater reuse of frequencies. Furthermore, the higher operational frequencies allow for more compact, by approximately a factor of two, antenna designs.
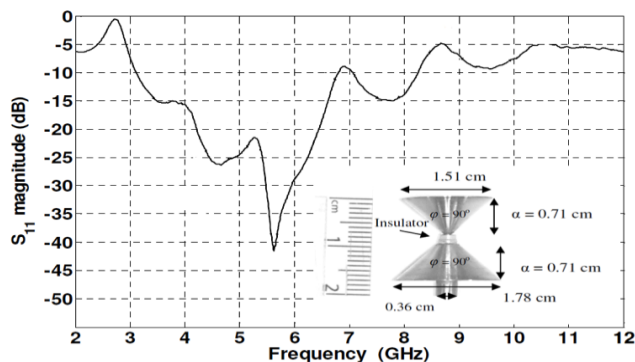

Figure 2. Bicone antenna design and S_{11} response [12].

Using a vector network analyzer (Agilent 8722ES), S_{21} data was collected between the receive antenna and the transmit antenna at 1601 points between 5.0 GHz and 6.0 GHz. Furthermore, this S_{21} data was collected at 1600 locations on a 40 by 40 horizontal grid at 3 mm intervals. The total physical extent by which the transmit antenna was moved corresponds to a 117 mm square (or ~2.2λ square at 5.5 GHz). This testing resulted in over 2.5 million S_{21} data points in total. We then repeated this procedure twice with the receive antenna rotated to two different and mutually cross-polarized orientations. That is, data was collected at three mutually orthogonal (in three-dimensions) linear polarizations.

Note that this data was from a single configuration of the reflecting plate in relation to the antenna (i.e., the environment was static). The conditions mimicked by this test set would be one where wireless sensor nodes are deployed, for example, in a star network where one node serves as a hub that collects or routes data from the other nodes. In this scenario, we envision the hub using a single, linearly polarized antenna and the other nodes using one or more mutually orthogonal, linearly polarized antennas. Alternatively, the multi-polarization antenna could be located at the hub but that may necessitate reconfiguring the antenna prior to communicating with the different distributed nodes, an approach tenable when polling for data but not necessarily when data is pushed to the hub.

B. Depolarization Effects

To illustrate the impact of depolarization caused by this test environment, we plot in Fig. 3 the median-normalized, cumulative distribution function, *cdf*, for the co-polarized S_{21} measurements at 5.2 GHz and at 5.8 GHz. The statistics, across the 1600 locations, for the data collected at 5.2 GHz are akin to the two-ray model proposed for enclosed environments [1]. At 5.8 GHz, the channel exhibited the most benign conditions over the 117 mm square area. In addition to the co-polarization data, we show the *cdf* for data taken at these same frequencies but with the receive antenna rotated to a horizontal (i.e., cross-polarized) position. We note that both frequencies now exhibit fading statistics closer to Rayleigh than for their co-polarized case. That is, the benign case now exhibits worse fading but the severe scenario is now less so.
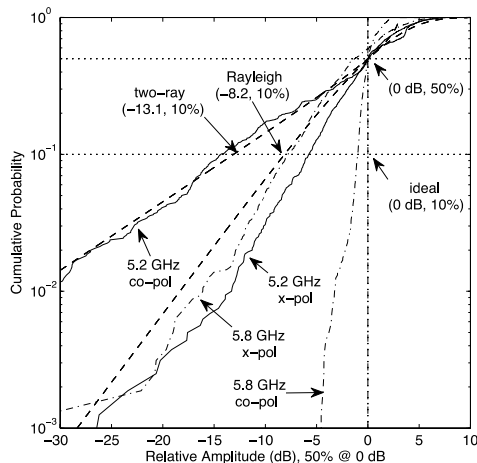
Figure 3. Representative data collected to show the effects of depolarization on both benign and severe channels. In both cases, the cross-polarized signal is more Rayleigh-like.

The median received power for the co-polarized and cross-polarized cases differ by only 1.25 dB for the 5.8 GHz case. We see this in Fig. 3 by the cross-polarization curve being shifted left at 50% on the y-axis. For the 5.2 GHz case this shift is negligibly (0.05 dB). However, significantly, the environment has nearly completely depolarized both the 5.2 GHz and the 5.8 GHz signals, resulting in near Rayleigh statistics. As a result of this near complete depolarization, we will investigate in §III the diversity gains achieved using three mutually orthogonal antennas under these channel conditions.

Fig. 3 represents just two of 1601 the frequencies measured. Frequency selective fading effects in this environment tend to be very narrowband and thus we should consider a more holistic view of the depolarization effects. For this, we leverage the 10% fade depth metric (10%FD) that was recently proposed for characterizing fading environments [13]. The 10%FD is that value (in dB) relative to the median received signal strength (or S_{21} value) below which the received signal falls for 10% of the measurements across time, space or frequency. In comparison to parametric models, the 10%FD has the advantage of being readily calculated from empirical data or found from *cdf* curves. For example, as seen in the *cdf* of Fig. 3, the 10%FD values corresponding to ideal, Rayleigh and two-ray channels are 0 dB, -8.2 dB and -13.1 dB, respectively. Also illustrated here is that the 10%FD metric is a single parameter that can characterize channels that are more benign than or worse than Rayleigh.

The 10%FD metric, calculated across space for each of the 1601 frequencies measured is shown as a *cdf* in Fig. 4 where for reference we also provide vertical markers for the Rayleigh and two-ray conditions. This curve indicates that for ~20% of the frequencies, the co-polarized measurements across space exhibited fading worse than Rayleigh (by the 10%FD metric). In addition, we see from this plot that fading environments ranging from the most benign (upper right point of the curve where the 10%FD = -1.0 dB) to extremely severe (lower left point where the 10%FD = -19.2 dB) occur over the very small area measured. These results are consistent with the constructive and deconstructive conditions intended by this test environment.
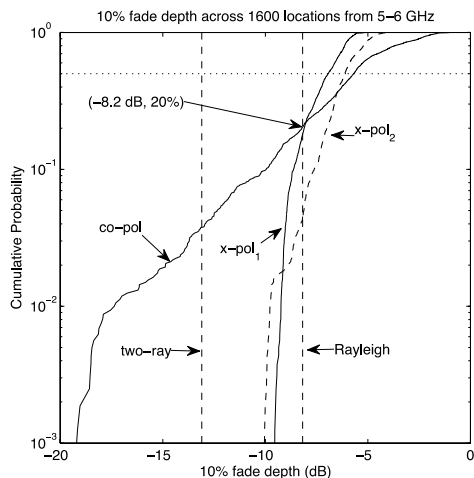
Figure 4. 10% fade depth of co-polarized and cross-polarized communication links across 1600 locations and 1601 frequencies between 5.0 and 6.0 GHz.

Also plotted in Fig. 4 is the *cdf* of the 10% fade depth found for our two different cross-polarization data sets. We see that the depolarization creates an environment that is more consistent (-10 dB < 10%FD < -4 dB) and more Rayleigh than was seen for the co-polarized case.

Our data S_{21} data (summarized in Table I) also shows that across the more than 2.5 million data points (1600 in space $\times$ 1601 in frequency) the mean cross-polarization discrimination (XFD) was only 2.3 dB for one cross-polarized orientation (x-pol$_1$) and 4.3 dB for the other (x-pol$_2$).

That is, there is, for the environment considered, some *average* power advantage to implementing co-polarized antennas. However, this advantage quickly disappears when one considers the probability of extremely deep fades as shown by the 10%FD. Thus, for the environment being characterized, much might be gained in overall link reliability if one could orient the receive antennas orthogonal to the transmit antennas. Whether this result is applicable to other severe fading environments remains to be shown. That being said, this result, however interesting, is unlikely to be of real practical use.

In particular, our data also shows significant change (i.e., > 20 dB) in the deepest of fades can occur over distances of 0.1λ or less. We contend therefore that it is not tenable to properly position in space or orientate in polarization an antenna with the expectation of achieving benign channel conditions for statically deployed devices. However, given the low XFD seen in this hyper-Rayleigh environment, we are motivated now investigate the effectiveness of diversity utilizing three mutually orthogonal antennas (i.e., a tri-polar design).

III. DIVERSITY RESULTS

At the onset, we noted our motivation was to consider harsh propagation environments in which future M2M devices will be deployed. Broad implementation of these devices, like with wireless sensors, necessitates that they be low-cost and therefore low in complexity.   As such, we now leverage means of mitigating severe channels that require minimal complexity and cost. In what follows, we investigate for our dataset three increasingly simple diversity schemes using $M = 3$ mutually orthogonal polarization configurations (i.e., a 3D tri-polar design) and compare their results.

A. Equal gain & selection combining

Equal gain combining (EGC) is the coherent summing of the signals received on all branches. For wireless sensors deployed in quasi-static environments, this technique could tenably be implemented using digitally controlled phase shifters. While not optimal relative to maximum ratio combining, EGC has the benefit of not adding the complexity of implementing and controlling multiple amplifiers. Our results in Fig. 5 (and in Table I) clearly show the benefit of $M = 3$ branch EGC in mitigating the deepest of fades created by our test environment. As the three branches exhibit greatly different fading and mean statistics, we have that the mean gain relative to the co-polarization case (7.5 dB) exceeds the theoretical 4.1 dB for i.i.d. conditions [5]. In addition, the mitigated environment is clearly Rician with K-factors that range from $K = $ ~3 dB to ~15 dB (by Fig. 4 in [11]).

An alternative and simpler approach for mitigating fading is selection diversity where only the single branch exhibiting the strongest response is chosen. The results for this technique are also shown in Fig. 5. We see that selection combining, like EGC, produces consistently better than Rayleigh channel conditions with Rician K-factors falling in the range of K = ~0 dB to ~15 dB. The mean diversity gain achieved using M = 3 selection diversity was found to be 1.4 dB. This gain falls short of that predicted for selection among M = 3 i.i.d. Rayleigh branches (i.e., 2.6 dB [5]). However, as illustrated in Fig. 4 and Table I, our three branches (one co-pol and two cross-pol) are far from i.i.d.
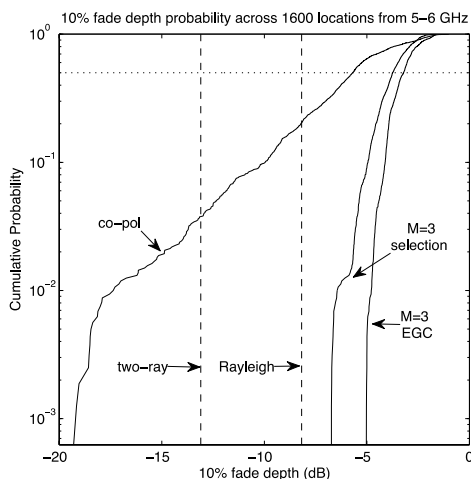

Figure 5. 10% fade depth of co-polarized link and results after M = 3 equal gain (EGC) and selection combining.

Selection combining can be readily implemented with current wireless sensor hardware [14] and the controlling algorithm could be greatly simplified, with slight performance degradation, by simply switching to a different antenna when the receive signal drops below a predefined threshold (i.e., switch combining). Such a simplification would still significantly improve the resulting fading statistics systems operating under hyper-Rayleigh conditions.

B. Passive polarization combining

The simplest diversity scheme for a M2M device to implement would require no computation. One such approach would be for a device to receive a signal that is the fixed summing of the three mutually orthogonal antennas. Clearly such a strategy is prone to produce both constructive and deconstructive effects on the received signal. However summing of three signals from different polarization paths could result in real and imaginary received voltage components tending towards Gaussian and therefore the resulting signal envelope, $\left|V_R\right|$, tending towards Rayleigh (one can readily verify this for three i.i.d. two-ray distributions). Given the severity of our co-polarization test environment, we viewed that an investigation of this simplest of techniques to be prudent. We see in Fig. 6 that passive combining does indeed result in somewhat more consistent and less severe channels as compared to the co-polarized link baseline. However, we also find that passive combining, for our test environment, has a mean diversity gain for our environment of -8.0 dB (Table I), which effectively negates any improvement seen in the fading. In short, even for our severe environment, we contend that this simplest of techniques offers no practical benefits for implementation in M2M systems. Furthermore, implementing a selection or switch diversity scheme adds little computational or hardware burden to a wireless device once the additional antenna branches needed for passive combining are in place and, as has been shown herein, results in significant improvement in channel characteristics, even with very compact antenna geometries.
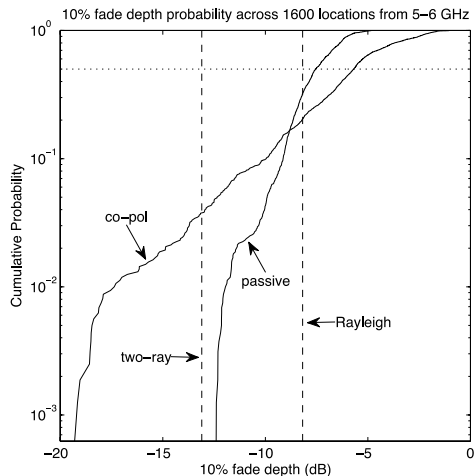
Figure 6. 10% fade depth of co-polarized link and results after $M = 3$ passive combining.

IV. CONCLUSION

We summarize the results of our investigation in Table I. Significantly, for the short (~1 m) link considered, we illustrated (1) the severity of fading that occurs for the co-polarized link; (2) the improvements seen by considering cross-polarized communications and (3) the effectiveness of implementing three possible diversity schemes using three, mutually orthogonal antennas. These results were obtained using very large data selects taken with fine spatial and frequency resolutions to fully capture the small-scale nature of fading produced in the test environment. To our knowledge, empirical results of this nature have not been presented to date. However, with the advent of M2M systems, we contend that further exploration of such confined/enclosed and reflective environments is warranted along with the development of easily manufactured and easily integrated tri-polar antenna designs to leverage the depolarization that, as has been illustrated, can be expected.

TABLE I. SUMMARY OF EXPERIMENTAL RESULTS.

Scenario (Figures)	Mean S_{21}	Min 10%FD	Max 10%FD	Worse than Rayleigh	Mean gain vs. co-pol
co-pol (3, 4, 5)	-44.2 dB	-19.3 dB	-1.0 dB	20.3%	n/a
x-pol$_1$ (3)	-46.5 dB	-9.6 dB	-5.1 dB	18.1%	-2.3 dB
x-pol$_2$ (3)	-48.5 dB	-10.1 dB	-3.9 dB	4.5%	-4.3 dB
EGC (4)	-36.7 dB	-5.0 dB	-1.6 dB	0%	+7.5 dB
Selection (4)	-42.8 dB	-6.7 dB	-1.6 dB	0%	+1.4 dB
Passive (5)	-52.2 dB	-12.4 dB	-4.8 dB	32.4%	-8.0 dB

REFERENCES

[1]   J. Frolik, "A case for considering hyper-Rayleigh fading channels," IEEE Trans. Wireless Communications, Vol. 6, No. 4, April 2007.

[2]   R. Ketcham, J. Frolik and J. Covell, "Propagation measurement and statistical modeling for wireless sensor systems aboard helicopters," IEEE Trans. Aerospace and Electronic Systems, Vol. 44, No. 4, October 2008.

[3]   V. Sipal, J. Gelabert, C. Stevens, B. Allen and D. Edwards, "Impact of confined environments on WiMedia UWB systems," 2011 Loughborough Antennas & Propagation Conference, Loughborough, UK, November 14-15, 2011.

[4]   V. Sipal, J. Gelabert, C. Stevens, B. Allen, and D. Edwards, "Adaptive OFDM for wireless interconnect in confined enclosures," IEEE Wireless Communications Letters, Vol. PP, No. 99, 2013.

[5]   A. Molisch, *Wireless Communications, 2 ed.* West Sussex, UK: Wiley & IEEE, 2011.

[6]   S.-C. Kwon and G. Stuber, "Geometrical theory of channel depolarization," IEEE Trans. Vehicular Tech., Vol. 60, No. 8, October 2011.

[7]   C. Oikonomopoulos-Zachos, "Double layer compact four-port antenna using a symmetrical feeding technique for future MIMO antenna systems at 5.6 GHz," IEEE Antennas and Propagation Society International Symposium (APSURSI), Toronto ON, July 11-17, 2010.

[8]   J. Griffin and G. Durgin, "Multipath fading measurements for multi-antenna backscatter RFID at 5.8 GHz," IEEE Int. Conference on RFID, Orlando FL, April 27-28, 2009.

[9]   K. Sivertsen, A. Liou and D. Michelson, "Depolarization of propagating signals by narrowband Ricean fading channels," IEEE Vehicular Technology Conference, Singapore, May 11-14, 2008.

[10] J. Frolik, "On appropriate models for characterizing hyper-Rayleigh fading," IEEE Trans. Wireless Communications, Vol. 7, No. 12, December 2008.

[11] G. Durgin, T. Rappaport, and D. de Wolf, "New analytical models and probability density functions for fading in wireless communications," IEEE Trans. Commun., Vol. 50, No. 6, June 2002.

[12] A. Kavatjikidis "Measurement Analysis and Capacity Performance of Ultra-Wideband Radio Propagation Channels," PhD. Thesis, University of Oxford, 2008

[13] J. Frolik, "A practical metric for fading environments," IEEE Wireless Communication Letters, Vol. 2, No. 2, April 2013.

[14] R. Ketcham and J. Frolik, "A low-complexity, compact antenna for mitigating frequency-selective fading," Sixth International Conference on Information Processing in Sensor Networks (IPSN), Cambridge, MA, April 25-27, 2007.